Robust High-Gain Loop-Shaping H_∞ Control of Servomechanisms

Chintae Choi* and Jong Shik Kim**

(Received April 29, 1996)

Loop-shaping H_∞ control with normalized coprime factorization is applied to a servo motor-driven precision positioning system. A high-gain controller is designed to attenuate the position errors caused by friction. The analysis of the controller shows that no limit cycle is introduced by the presence of actuator saturation. The designed H_∞ control system is experimentally tested on a rotary index table which requires a high-accuracy position control. The results show that the suggested control scheme improves the positional accuracy and its robustness to the model perturbation and external disturbances without any compensation scheme for friction.

Key Words : Robust, H_∞, Control, Precision, Position.

1. Introduction

High-speed/high-accuracy position-control systems are indispensible to the improvement of productivity as well as to the manufacture of precision products. While commonly neglected, because it is difficult to model and poorly understood, friction is present to some degree in all mechanical systems, and continues to impose limits on performance. Mechanical systems are distinguished from other controlled plants by the presence of several significant nonlinearities such as static friction, Coulomb friction, backlash and actuator saturation. Among these nonlinearities, backlash may be reduced at the expense of increased stiction and Coulomb friction. The discontinuous nature of Coulomb-type friction near zero velocity causes stick-slip behavior which limits the fidelity of position and force control. As the performance criteria, such as cycle time, are made more stringent, the dynamic load dependency of friction becomes more influential. Stiction may cause steady-state error, or limit cycle near the reference position in the linear control of positioning system. Failure to account for the effects of friction can lead to tracking errors and oscillation.

An adaptive pulse-width control scheme was proposed to achieve precise positioning in the presence of stiction and Coulomb friction (Yang and Tomizuka, (1990)). It is intended to be used near the reference position. Any conventional control law can be applied, until the system sticks near the reference position. When a motion stops and the error remains, a functional relationship between the pulse width and the error is updated by an adaptive algorithm, and a new pulse is applied. This sequence continues until the motion comes to a stop with zero error. The adaptive friction compensation at low velocities has been dealt with (Canudas de Wit, et al., (1991)) and a simple model, linear in parameters, that captures the downward bends at velocites close at zero was proposed.

Ruina (1980) worked on the experimental and theoretical development of constitutive frictions, and suggested state variable friction models through experiments on rock samples, with and without lubricants. The ramifications of transient friction behavior as expressed by a state variable friction law for the control of low-velocity motion has also been explored (Dupont, (1991)). A

* Process Automation Team, RIST, Pohang, 790-330, Korea
** School of Mechaical Engineering, Pusan National University, Pusan, 609-735, Korea

repititive control (Tung, et al., (1993)), a kind of learning control, was applied to compensate for stiction-induced errors which was a source of contouring errors in machine-tool systems.

Ohnishi (1987) proposed a two-degree-of-freedom controller using a disturbance observer. It estimates the disturbance and cancels the actual disturbance with the estimate. This method has a similar control structure to that of time delay control (Youcef-Toumi and Ito, (1990)) and time delayed uncertainty cancellation (Hsia, et al., (1991)) in that the internal loop has a infinite loop gain as delay time becomes infinitely small. Lee and Tomizuka (1994) designed a control scheme for perfect tracking of a positioning system. The excellent performance achieved for certain parametric variations and external disturbances is due to an infinitely large bandwidth. Since the large bandwidth is inherent to the characteristics of the structure of the disturbance observer, this kind of the controller is very sensitive to measurement noise and is not robust against dynamic model uncertainties (Liang and Looze, (1992)).

The normal forces orthogonal to the moving direction of the servomechanism, which determine the friction, constantly vary according to the temperature changes in the moving contacts and inertia perturbations of the masses attached to the moving mechanisms such as linear slide tables, index table, and so on. Beginning with Sampson, et al. (1943) and Rabinowitz (1959), it was noted that friction is not determined by the current velocity alone; it depends on the history of the motion and the instantaneous velocity change. In the environments where the dynamic normal force and the velocity direction are varying, it is very difficult to obtain an accurate model to completely cancel the effects of friction in servo systems. Therefore, it is more realistic to attenuate bounded friction sufficiently to the desired magnitude level than to resort to model-based compensation.

This paper proposes an H_∞ control scheme to compensate for the external disturbances including friction through a high-gain controller. The proposed scheme consequently controls the desired positions of servomechanisms accurately since positional errors are inversely proportional to the gain of the feedback controller. The high-gain controller results from a loop compensator with a large gain being selected in loop shaping so that the sensitivity function may have a small magnitude in the low-frequency region. Though the high-gain controller immediately saturates the actuators, the saturation does not give rise to a severe stability problem under the condition that the unstable poles and integrators are not included in the SISO closed-loop system. The designed high-gain controller has been tested experimentally on a rotary index table which requires a high-accuracy position control. To check for robust performance when parametric modelling errors exist, the tests were repeated with load variations.

2. Robust Controller Design Using Loop-Shaping

2.1. Normalized coprime factorization stabilization

Let the nominal $p\times m$ system, G, has a minimal state-space realization and normalized coprime factorization (NRCF) such that

$$G(s)=C(sI-A)^{-1}B \tag{1}$$

and

$$G(s)=NM^{-1} \tag{2}$$

Definition 1 : A right coprime factorization of G is normalized if the matrix $[N^TM^T]^T$ is inner. If X and Y$>$0 are the solutions to the Riccati equations (Meyer, 1987)

$$\begin{aligned} 0&=A^TX+XA-XBB^TX+C^TC \\ 0&=AY+YA^T-YC^TCY+BB^T \end{aligned} \tag{3}$$

then the matix $[N^T\ M^T]^T$ is easily determined from the following state-space realization.

$$F=-R^{-1}B^TX\begin{bmatrix}N\\M\end{bmatrix}=\left[\begin{array}{c|c} A+BF & B \\ \hline C & O \\ F & I \end{array}\right] \tag{4}$$

Then, any other perturbed system of the same input/output dimensions can be written in the

form

$$G_\epsilon := (N+\Delta_N)(M+\Delta_M)^{-1} \tag{5}$$

where Δ_N, and $\Delta_M \in H_\infty$ are stable transfer functions. The robust stabilization problem is to stabilize the nominal system, G, with NRCF(N, M) and the family of systems G_ϵ using a proper feedback controller K.

Definition 2 (NRCF Robust Stabilization): Let (N, M) be a NRCF of G, then 1) Find the largest positive number ϵ_{max} called the maximum stability margin, such that (N, M, ϵ_{max}) is robustly stable. 2) For a particular value $\epsilon \leq \epsilon_{max}$, synthesize a feedback controller, K, such that (N, M, K, ϵ) is robustly stable.

The upper linear fractional transformation and lower linear fractional transformation can be defined for this problem.

$$F_u(P, \begin{bmatrix} \Delta_N \\ \Delta_M \end{bmatrix}) := (N+\Delta_N)(M+\Delta_M)^{-1} \tag{6}$$

$$F_l(P, K) := M^{-1}(I-KG)^{-1}[K\ I] \tag{7}$$

The problem fits neatly into the standard H_∞ framework. The feedback system $F_l(F_u, K)$ is stable for all $\Delta_N, \Delta_M \in H_\infty$ if $F_l(P, K) \in H_\infty$ and $\|F_l(P, K)\|_\infty \leq \epsilon^{-1}$ by the small-gain theorem. By multiplying the expression for $F_l(P, K)$ on the left by the inner transfer function $[N^T M^T]^T$, a two-block H_∞ problem is written as a four-block H_∞ problem. Rephrasing this, the solution of the problem is given by minimizing

$$\epsilon_{max}^{-1} = \inf_K \left\| \begin{bmatrix} G \\ I \end{bmatrix} (I-KG)^{-1}[K\ I] \right\|_\infty \tag{8}$$

where ϵ_{max} is the maximum stability margin such that (N, M, ϵ_{max}) is robustly stable. The above equation is also expressed as

$$\epsilon_{max}^{-1} = \inf_K \left\| \begin{bmatrix} G(I-GK)^{-1}K & G(I-GK)^{-1} \\ (I-GK)^{-1}K & (I-GK)^{-1} \end{bmatrix} \right\|_\infty \tag{9}$$

Minimizing the norm of the complementary sensitivity function, $G(I-GK)^{-1}K$ indicates robust stability for the multiplicative uncertainty. $G(I-GK)^{-1}$ and $(I-GK)^{-1}$ are the transfer functions from the disturbance reflected to the control input and reference input, respectively. It can be conjectured that the closed-loop system has good performances for disturbance attenuation and command following. The maximum stability margin ϵ_{max} is obtained from the Nehari extension (McFarlane and Glover, (1992))

$$\epsilon_{max} = \{1 - \left\| \begin{bmatrix} N \\ M \end{bmatrix} \right\|_H^2\}^{1/2} \tag{10}$$

where $\|\cdot\|_H$ denotes the Hankel norm. A state-space realization of the central controller satisfying the stability margin is

$$K = \left[\begin{array}{c|c} A+\Phi+\epsilon^{-2}W_l\Omega C & \epsilon^{-2}W_l\Omega \\ \hline B^T X & 0 \end{array}\right] \tag{11}$$

where $W_l = ((1-\epsilon^{-2})I + YX)^{-1}$, $\Phi = BB^T$ and $\Omega = YC^T$. This method has a remarkable characteristics in synthesizing the optimal control directly from the Nehari extension of the normalized right coprime factorization of the nominal system, while other H_∞ syntheses require iterative procedures to obtain optimal or suboptimal solutions to satisfy the H_∞ norm.

2.2. Loop-shaping techniques

In loop-shaping design, the closed-loop design objectives are specified in terms of requirements on the open-loop singular values of the compensated system. For example, given a sysem G and compensator K, a typical design objective is that $\bar{\sigma}((I-GK)^{-1})(j\omega)$ is small in order to achieve good performance, and $\bar{\sigma}(GK(I-GK)^{-1})$ is small for good stability properties. Noting that performance is usually required at low frequencies, and robustness at high frequencies, a designer specifies closed-loop objectives in terms of requirements on the open-loop singular values of the compensated system.

2.2.1 The loop-shaping design procedure

(1) Loop Shaping: using a loop compensator, W, the magnitude of the nominal system G is shaped to give a desired target loop which determines the open-loop shape of the closed-loop system. The selection of the target loop uses familiar SISO loop-shaping guidelines. Shaping a crossover roll-off rate close to -20dB/ dec is consistent with Bode's observation that roll-off rate determines phase, and that a rate of -20dB/ dec corresponds to 90 degrees of phase. The

actual system can be unstable, if the roll-off rate is -40dB/dec. The nominal system and the loop compensator, W, are combined to form the shaped system, G_s, where $G_s = GW$.

(2) Robust Stabilisation: a feedback controller, K_∞, is synthesized using the NRCF stabilization procedure which robustly stabilizes the NRCF of G_s with stability margin.

(3) The final feedback controller, K, is then constructed by combining the H_∞ controller, K_∞, with the loop compensator W such that $K = WK_\infty$.

"Stability margin", ϵ has two meanings in this design procedure. Firstly, treats ϵ as an indicator of the success of the loop shaping. ϵ captures information on the compatibility of the desired loop-shape with the stability constraints. Secondly, ϵ can be interpreted as a measure of robustness. It provides direct information on the size of the neighbourhood of plants close to the shaped plant in the gap metric that are also stabilized by the controller (Georgiou and Smith, 1987).

3. Analysis of the High-Gain Controller

The next step is to deal with the position control system forced by the friction forces illustrated in Fig. 1. All the signals are multivariable, in general, and both nominal models for G and K are finite-dimensional linear time-invariant systems. The friction forces, f, have bounded energy in the low- frequency region, y are the outputs equivalent to the position signal, v are velocity signals, and s is a Laplacian operator. Obtaining the the error signals to the friction force,

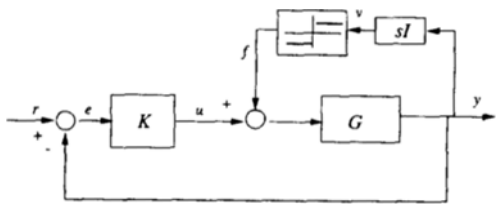

Fig. 1 The standard feedback system with friction.

$$e = (I + GK)^{-1}Gf \tag{12}$$

the norm of errors is

$$\begin{aligned} \|e\| &= \|(I + GK)^{-1}Gf\| \\ &\leq \|(I + GK)^{-1}G\|\|f\| \end{aligned} \tag{13}$$

If Euclidean norm is used for e and f,

$$\|(I + GK)^{-1}G\| = \bar{\sigma}((I + GK)^{-1}G) \tag{14}$$

where $\bar{\sigma}$ denotes the maximum singular value. At low frequencies such that $\underline{\sigma}(GK) \gg 1$, the approximations

$$\bar{\sigma}((I + GK)^{-1}G) \cong 1/\underline{\sigma}(K) \tag{15}$$

can be made.

Since $\bar{\sigma}(K) = \underline{\sigma}(K) = |K(j\omega)|$ in SISO case, Eq. (13) can be written as

$$\|e\| \leq (1/|K(j\omega)|)\|f\| \tag{16}$$

Therefore, tracking errors caused by the friction forces are inversely proportional to the magnitude of the frequency response in the low-frequency region, and the errors can be sufficiently attenuated by a feedback controller having a high gain in this frequency. A loop compensator with a large proportional gain is selected to obtain the high-gain ontroller when an H_∞ controller is designed using the loop-shaping approch.

Since the electrical time constant is much smaller than the mechanical time constant in the servomotor-driven position control system, the armature inductance effect can be neglected. Therefore, the dynamic model of the system, whether it has rotational joints or translational ones, is, in general, characterized by the 2nd-order transfer function, and has no finite zeros. Because the relative order of the transfer function is 2, the roll-off rate of its magnitude near the crossover frequency is -40dB/dec. For the target loop to have 20dB/dec. in the crossover frequency, it is necessary to insert a finite zero as a loop compensator, which guarantees a good phase margin and robust stability. The proportional gain and the locations of the zero are determined by the desired error magnitude, the magnitude of the friction force and a roll-off rate of the unshaped open-loop Bode plot. The gain is approximately calculated by Eq. (16). This gain is slightly changed in the final controller by inclusion of the H_∞

controller, which causes deterioration in the open-loop shape, but the degradation in the loop shape caused by the H_∞ controller, K_∞, is limited at frequencies where the specified loop shape is sufficiently large or sufficiently small. Since the poles and zeros in the H_∞ controller are mostly located near or beyond the crossover frequency, and the controller is strictly proper as expressed in the state-space model of the controller, it has a higher roll-off rate in the high frequencies and good noise immunity.

The stability margin, ϵ, is also a factor in determining the magnitude of the H_∞ controller, K_∞. As ϵ becomes smaller, the deterioration in the target shape is enlarged. But as the H_∞ controller maintains its magnitude near 1 in the low-frequency range, the final controller approximately inherits its gain from the proportional gain of the loop compensator. The high-gain scheme immediately saturates the actuators. In multivariable systems, saturation affects to both the magnitude and the direction of singular values. The loss in directionality can break the performance of decoupling between outputs. In particular, anti-windup must be considered in the feedback controller with integrators when the actuators saturate.

The saturation does not bring about a severe stability problem in a SISO system, which has no unstable poles and integral compensators. Robust stability is examined by experimental results in the Sec. 5. Actuator saturation primarily affects the transient performance, and deteriorates the speed of response. The describing function, $N(M)$, for the saturation is given as

$$N(M)=\frac{2k}{\pi}\left[\sin^{-1}\left(\frac{a}{M}\right)+\frac{a}{M}\sqrt{1-\frac{a^2}{M^2}}\right] \quad (17)$$

where M, a, and k denote the control input to the actuator, the range and the slope of the linearity, respectively. If $M \leq a$, then $N(M)=1$, and the input remains in the linear range. The magnitude of the control input for cancelling friction force, in most cases, is within the linear range, not saturation range, and therefore, saturation does not degrade the capabilities for error attenuation. The existence of limit cycles caused by the saturation must also be investigated. A describing function is mainly used in predicting the limit cycles in nonlinear systems. Obtaining the relationship between a linear part and the describing function from the characteristic equation of the closed-loop system with actuator saturation,

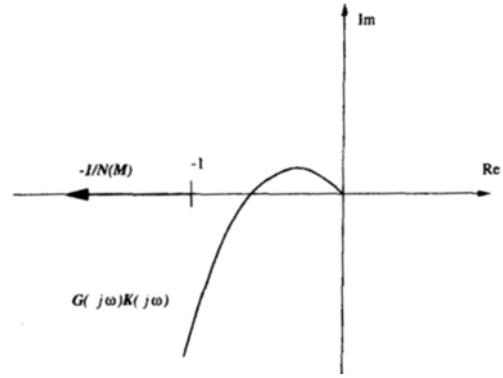

Fig. 2 Plot of $-1/N(M)$ and $G(j\omega)K(j\omega)$.

$$G(j\omega)K(j\omega)=-\frac{1}{N(M)} \quad (18)$$

The servomechanism, as mentioned above, is a stable 2nd-order system without finite zeros, and it is assumed that $K(j\omega)$ is a stabilizing controller for the closed-loop system, andhas no finite zeros in the right half of the s-plane. Then, the locus of $G(j\omega)K(j\omega)$ does not encircle the -1 point of the real axis. As M varies from 0 to ∞, the locus of $-1/N(M)$ starts from the -1 point on the real axis and extends to $-\infty$. The frequency response function $G(j\omega)K(j\omega)$ and the negative inverse describing function $-1/N(M)$ can be plotted in the complex plane, as shown in Fig. 2. The loci of $-1/N(M)$ and $G(j\omega)K(j\omega)$ do not intersect each other in this figure, which means that limit cycles caused by the actuator saturation will not exist. Therefore, the high-gain controller does not introduce stable oscillation.

4. Design of the Proposed Controller

Figure 3 shows a testbed for high-accuracy position control. The system consists of two main elements: the servomotor-driven index table and a VME computer with interface. The resolution of

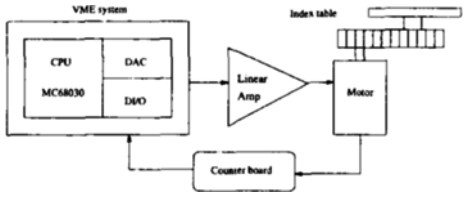

Fig. 3 Experimental setup of the servomechanism.

the position sensor, which is an incremental encoder, is 5.992×10^{-6}rad. The motor used is a DC servo motor, and the controller is implemented using an MVME143 computer that has a VME bus and a 32-bit microprocessor, MC68030, running at 25MHz. The computer is interfaced to a power amp via a DAC board and to an encoder through a counter board. The numerical values of the electrical and mechanical parameters of the used motor are listed in Table 1.

Table 1 Specifications of the motor

Motor model(Tamakawa)	TS1980
Moment of inertia	0.28 kg cm^2
Output power	100 **W**
Mechanical time constant	3.9 ms
Electrical time constant	0.98 ms
Peak torque	18.4 kg cm
Gear ratio	10:1
Maximum speed	1500 rpm

The H_∞ controller designed in the continuous-time domain is transformed to a discrete-time domain controller through bilinear transformation. The digital codes were written in C for the actual control, and they are executed every 2 msec under the assistance of a real-time operating system VMEexec. It is an important requirement for a microprocessor-based control system, and has real-time kernel and software development environments. It is assumed that the transfer function of the index table is a 2nd-order system, as stated above. The transfer function for the index table is approximately given as follows:

$$G(s)=\frac{k}{s(Ts+1)} \tag{19}$$

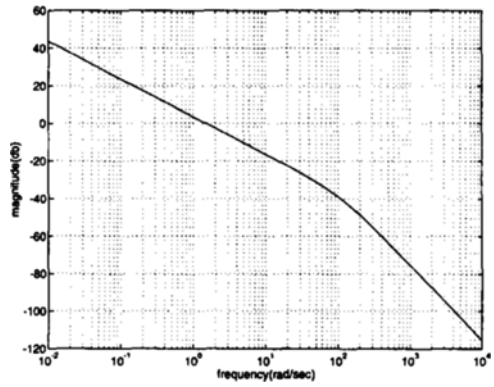

Fig. 4 The open-loop frequency response of the index table.

where k is 1.52 and T is 0.009 sec. The estimated friction force is 0.004 volts. Since the index table is designed for high-accuracy operations, it has a high power transmission ratio and small friction. The open-loop Bode plot for $G(s)$ is shown in Fig. 4. The roll-off rate in the crossover frequency is -20 db/dec. But if a large proportional gain is used in the feedback controller, the shape necessarily goes up, and the roll-off rate in the crossover frequency will be -40 db/dec. So the insertion of a finite zero near the crossover frequency guarantees that the target loop will have -20dB/dec. The shaped plant $G_s(s)$ is obtained by inserting a loop compensator, $k_p(s/\omega_z+1)$, where 105 rad/sec. is assigned to ω_z. An ω_z much larger than the natural frequency, 1/0.009, can not transform the roll-off rate near the crossover frequency, and an ω_z smaller than that natural frequency reduces the bandwidth of the closed-loop system. The k_p is chosen to be 70 to sufficiently attenuate the position errors. Saturation level to the linear amp is set to 5 volts to test the characteristics of the high-gain controller, and this corresponds to the great high gain, compared to the linear range of the linear amp. The shaped transfer function is

$$G_s(s)=\frac{kk_p(s/\omega_z+1)}{s(Ts+1)} \tag{20}$$

A stabilizing controller for the shaped plant is synthesized with a appropriate stability margin in the following step. The maximum stability margin is 0.72 which is calculated by Eq. (10). The

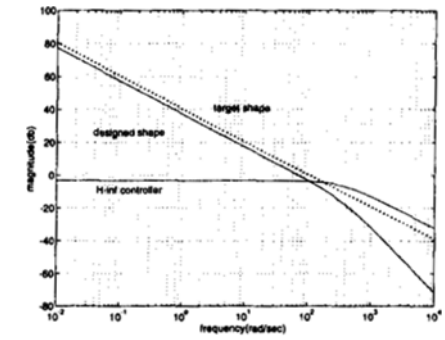

(a) Magnitudes

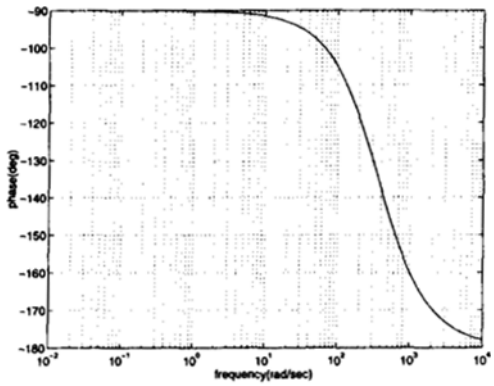

(b) Phase

Fig. 5 Bode plot of the loop gain GK.

stability margin ϵ near to ϵ_{max} gives good loop recovery, but has a disadvantage to introduce fast poles. Here, the H_∞ controller, K_∞, is designed with stability margin $\epsilon=0.53$ to prevent fast poles from being introduced to the H_∞ controller. The final feedback controller K is obtained by combining the loop compensator and K_∞.

$$K(s)=WK_\infty(s)$$
$$=\left[\begin{array}{cc|c} -466 & -37958 & 1 \\ 1 & 0 & 0 \\ \hline -40600 & -4268900 & 161 \end{array}\right] \quad (21)$$

The frequency responses of the target loop, the designed loop shape and the controller K_∞ are shown in Fig. 5. The designed loop gently crosses the 0 db with -20dB/dec., and therefore it will have a nice transient response. It also illustrates a higher roll-off rate in the higher-frequency region and therefore robustness to the measurement noise. This shape well satisfies the requirements that the open-loop shape in the low-and high-frequency regions needs to meet the closed-loop performance. The magnitude of the H_∞ controller is slightly below 0 db in the low-frequency region because of a smaller ϵ than ϵ_{max}. This magnitude will gradually approach 0 db, if a larger $\epsilon$is adopted.

Relative stability given by the gain and phase margins in SISO system, to some extent, implies robustness of the system. Sufficiently large gain and phase margins are necessary for the system to have good relative stability. The stability margin, $\epsilon=0.53$, appears to give good loop recovery, because the designed loop has slightly lower gain than the target loop. This results from the selection of an ϵ which is smaller than ϵ_{max}. The gain and phase margins of the compensated system are about 168 db and 78 degrees, respectively. The gain and phase margins of the compensatedsystem mean that $G(j\omega)K(j\omega)$ does not encircle the -1 point on the real axis in the complex plane. Therefore, no limit cycle exists in the closed-loop system, as described in the previous section.

5. Experimental Results

This section details actual experimental results obtained using the previously described system. A step response experiment is carried out to demonstrate the effectiveness of the proposed controller. Step responses are useful information to examine the disturbance attenuation of the controller. The index table is given a 0.4 radians step command, which corresponds to a fairly large command, to check characteristics of the high-accuracy position-control system. In the digital implementation, the control law is

$$u(k)=1.3u(k-1)-0.4u(k-2)+117e(k)$$
$$-188.8e(k-1)+76e(k-2) \quad (22)$$

where u and e are the control input to the DAC and position error.

Robust performance of the high-gain controller to be examined is the ability to reject load uncertainty which causes a parametric modelling error, and results in a shift of pole locations and a plant gain change. The friction force is also changed to

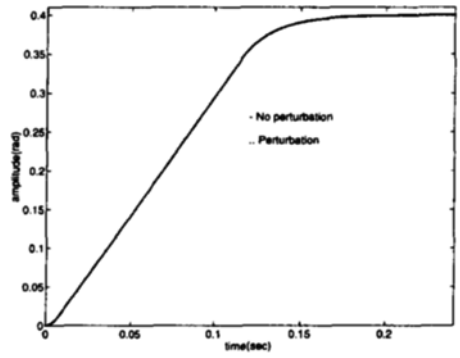

(a) Position responses

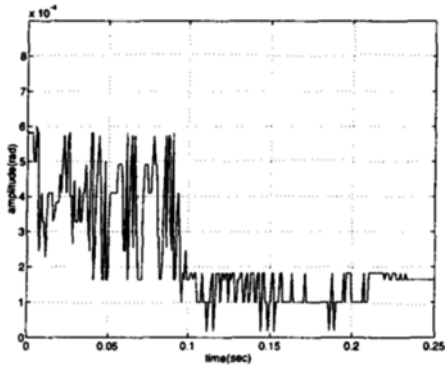

(b) Positional error difference by the mass

Fig. 6 The step responses with/without the mass.

a higher level. To demonstrate this, the experiments are repeated with a 6 kg load attached to the index table. The moment of inertia of the load is about 45 $kgcm^2$. Figure 6(a) shows the position responses with/without the load. The difference of positional error between the cases with/without the attached mass is shown in Fig. 6(b). The steady-state errors are about 1×10^{-5} and 1.7×10^{-4} radians without/with the mass, respectively. The slightly larger positional error in the transient stage is due to the increased inertia and friction of the index table. The angle errors illustrate a good performance for the load perturbation. It is shown that the steady-state errors for the friction are adequately attenuated by the high-gain controller, as expected. Smaller errors are anticipated if a position sensor having a higher resolution is used.

For comparison purpose, a PID controller for improving steady-state response is also designed without any feedforward compensation for friction, because it is difficult to obtain its accurate model. Figure 7 is phase plot of the response to the step position reference. The dotted line indicates phase plane response of the H_∞ controller and it has no oscillations. Integral-action in the PID controller causes a stable limit cycle near the reference position by friction, though it gives a slightly smaller steady-state error than the H_∞ controller.

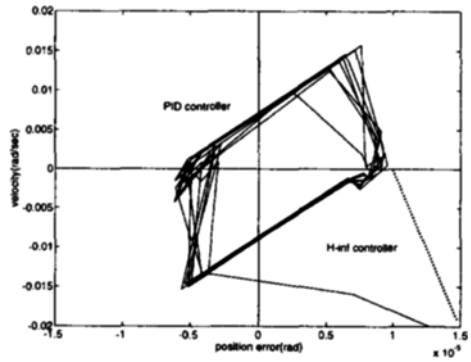

Fig. 7 Phase plot of the responses for the PID and H_∞ control.

Tracking performances of two controllers are compared: one with the H_∞ controller and the other with the PID controller. The trajectory used in the experiments to check the tracking performance is a fifth-order polynomial curve as shown in Fig. 8. This trajectory corresponds to a 1 radian angle and 0.8 sec transition time. While tracking error with the PID controller remains below 6.2×10^{-3} radians, the H^∞ one generates the maximum tracking error less than 5.1×10^{-3} radians and this is a small tracking error. The H_∞ controller shows better tracking performance than the PID one.

One of the major concerns for the high-gain controller is its performance under actuator saturation. To address this concern, the output of the controller and the saturated control signal are shown in Fig. 9 where the index table is given a 0.4 radians step command. The motor is saturated for a control signal magnitude beyond 5 volts, which is indicated by the dotted line on the plot, because linear characteristics of the power amp for the control input ranges from -5 volt to +5 volt. Saturation corresponds to utilize maximal

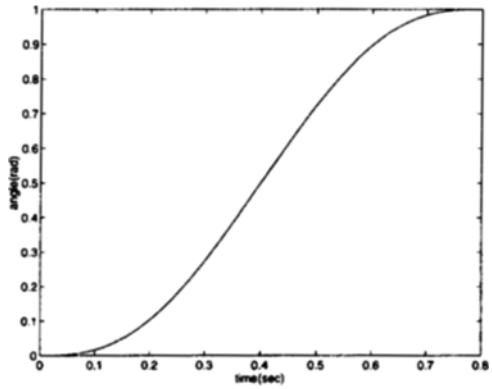

(a) Desired trajectory

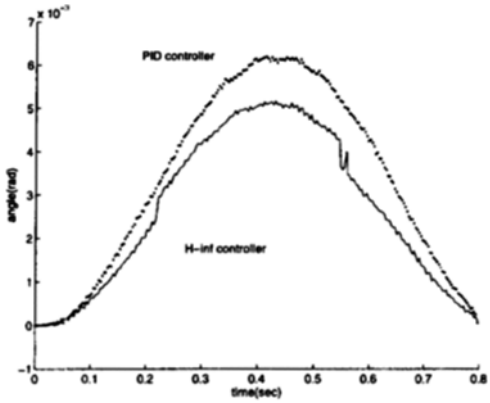

(b) Traking errors

Fig. 8 Tracking responses.

power of the motor amp. The motor is always saturated in the initial stage, and encouraged to response rapidly to the desired reference.

The ability to reject the external disturbance is also important for the controller to have the applicability to the real system. The external disturbances are tested by an elastic spring that is physically attached to the index table, as shown in Fig. 10. The torques induced by the spring have characters of varying disturbances, but they have energies in the low frequencies region. Therefore, they can also be attenuated by a high-gain H_∞ controller.

Two experiments are repeated with different spring forces. While the index table rotated 0.4 radians, the spring forces varied linearly from 1.5 kg_f to $2.5kg_f$ in the first experiment and from 2. $6kg_f$ to $3.5kg_f$ in the second. The final opposed torques caused by the attached spring are 16 kg_fcm and $23.5kg_fcm$ in the above two experiments, respectively. The peak torque of the mechanism is around $167.44kg_fcm$ which is 0.91 (transmission ratio)$\times$10 (gear ratio)$\times$18.4(the peak torque of the used motor). The maximum torque by the spring corresponds to 14 % of the peak value of the system and this is a big disturbance in the practical applications of high-precision positioning systems. These torques, in general, degrade the transient responses and give rise to large steady-state errors.

Figure 11 shows differences of the positional errors between the cases with two opposed torques and the one without any disturbance.

Though the errors by the spring torques increase in the transient stage, the controller still shows good steady-state rsponses despite the exteral spring torque.

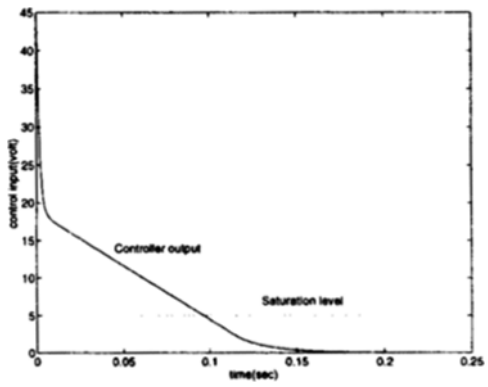

Fig. 9 The controller output with actuator saturation.

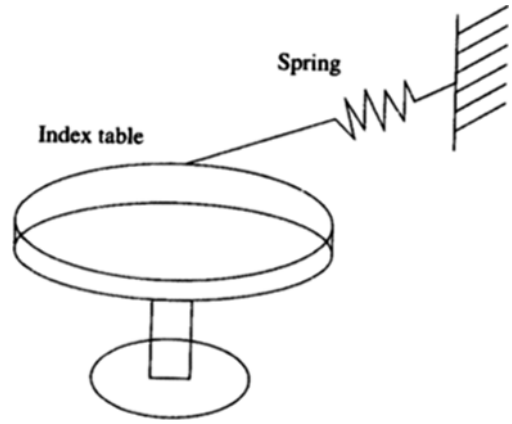

Fig. 10 The index table pulled with a coil spring.

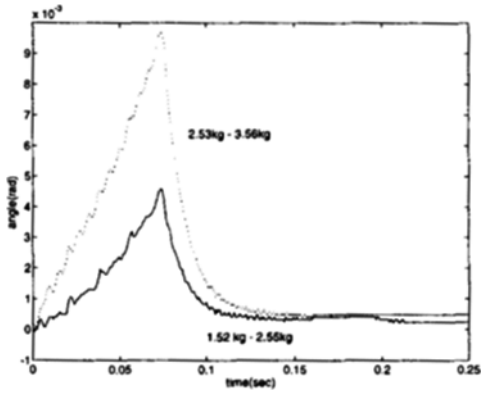

Fig. 11 The error differences caused by disturbances.

6. Conclusion

Friction causes steady-state position errors or tracking lags in servomechanisms. It is necessary to control the postions precisely, without introducing any stable oscillations near the reference position in the existence of friction and disturbances. A design method for a robust motion controller based on high-gain loop-shaping synthesis has been presented in this paper. It was applied to an index table requiring high-accuracy position control. The loop-shaping method with H_∞ synthesis provides ease and flexibility in designing a controller which meets the specifications. The high-gain loop-shaping scheme shows that the designed controller is effective in attenuating the friction forces to the desired magnitude.

The performance of the controller has been examined through experiments under various load uncertainties and disturbances, including friction. The positional error due to the effect of the friction in the index table was greatly reduced using a suboptimal controller without any feedforward friction compensation. The experimental results demonstrated that the saturation caused by the high-gain contoller does not break nominal and robust stability. The high-gain controller does not completely eliminate the positioning errors caused by friction, but it can reduce the errors to a sufficiently small level. Moreover, it has the robustness to the model perturbation, noise immunity and disturbance insensitivity which a real-world controller must possess. Superior performance may be obtained if a more accurate position sensor is used.

References

Canudas de Wit *et al.*, 1991, "Adaptive Friction Compensation in Robot Manipulators: Low Velocities," *The International Journal of Robotics Research*, Vol. 10, pp. 189~199.

Dupont, P. E., 1991, "Avoiding Stick-Slip in Position and Force Control Through Feedback," *Proceedings of the 1991 IEEE Int. Robotics and Automation Conf.*, Sacramento, pp. 1470~1475.

Georgiou, T. and Smith, M. , 1987, "Optimal Robustness in the Gap Metric," *IEEE Trans. on Automat. Contr.* , Vol. 30, pp. 555~565.

Hsia, T. C., Lasky, T. A. and Guo, Z., 1991, "Robbust Independent Joint Controller Design for Industrial Robot Manipulators," *IEEE Trans. Industrial Electronics*, Vol. 38. pp. 21~25.

Lee, H. S. and Tomizuka, M., 1994, "Design of Friction-Compensated and Robust Digital Tracking Controllers for High-Accuracy Positioning Systems," *Proceedings of the 1994 Japan-USA Symposium on Flexible Automation*.

Liang, Y. and Looze, D. P., 1992, "Evaluation of Time-delayed Uncertainty Cancellation Systems," *Proceedings of the ACC*, pp. 1950~1954.

McFarlane, D. C. and Glover, K., 1992, "A Loop Shaping Design Procedure Using Synthesis," *IEEE Trans. on Automat. Contr.*, Vol.37, pp. 759~769.

Meyer, D., 1987, Model Reduction via Fractional Representation, Ph.D. thesis, Stanford University.

Ohnishi, K., 1987, "A New Servo Method in Mechatronics," *Trans. JSEE*, Vol. 107-D, pp. 83~86.

Rabinowitz, E., 1959, Study of the Stick-Slip Process, *Friction and Wear*, Ed. Robert Davies, Elsevier Publishing Co.,New York.

Ruina, A., 1980, Friction Laws and Instabilities: A Quasistatic Analysis of Some Dry Fric-

tional Behavior, Ph.D. Dissertation, Brown University.

Sampson, J. et al., 1943, "Friction behivior During the Slip Portion of the Stick-Slip," *Process. J. of Applied Physics*, Vol.14, pp. 689~700.

Tung, E. D. et al., 1993, "Low Velocity Friction Compensation for Machine Tool Feed Drves," *Proceedings of the ACC*, San Francisco, pp. 1932~1936.

Yang, S. and Tomizuka, M., 1988, "Adaptive Pulse Width Control for Precise Positioning Under the Influence of Stiction and Coulomb Friction," *ASME, Journal of Dynamic Systems, Measurement, and Control*, Vol. 110, pp. 221~227.

Youcef-Toumi, K. and Ito, O., 1990, "A Time Delay Controller for Systems With Unknown Dynamics," *ASME, Journal of Dynamic Systems, Measurement, and Control*, Vol. 112, pp. 133~142.